



Cite this: *RSC Adv.*, 2018, 8, 38891

# Scope of sulfur dioxide incorporation into alkylallyldiallylamine–maleic acid–SO<sub>2</sub> tercyclopolymer†

Ibrahim Y. Yaagoob, Shaikh A. Ali, \* Hasan A. Al-Muallem \* and Mohammad A. J. Mazumder

Alternate copolymerization of diallylamine derivatives [(CH<sub>2</sub>=CH–CH<sub>2</sub>)<sub>2</sub>NR; R = Me, (CH<sub>2</sub>)<sub>3</sub>PO(OEt)<sub>2</sub>, and CH<sub>2</sub>PO(OEt)<sub>2</sub>] (I)–maleic acid (MA) and (I·HCl)–SO<sub>2</sub> pairs have been carried out thermally using ammonium persulfate initiator as well as UV radiation at a λ of 365 nm. The reactivity ratios of ≈0 for the monomers in each pair I–MA and I·HCl–SO<sub>2</sub> ensured their alternation in each copolymer. However, numerous attempted terpolymerizations of I–MA–SO<sub>2</sub> failed to entice MA to participate to any meaningful extent. In contrast to reported literature, only 1–2 mol% of MA was incorporated into the polymer chain mainly consisting of poly(I–alt–SO<sub>2</sub>). Quaternary diallyldialkylammonium chloride [(CH<sub>2</sub>=CH–CH<sub>2</sub>)<sub>2</sub>N<sup>+</sup>R<sub>2</sub>Cl<sup>–</sup>; R = Me, Et] (II) also, did not participate in II–MA–SO<sub>2</sub> terpolymerizations. Poly((I, R = Me)–alt–SO<sub>2</sub>) (III) is a stimuli-responsive polyampholyte; its transformation under pH-induced changes to cationic, polyampholyte-anionic, and dianionic polyelectrolytes has been examined by viscosity measurements. The pK<sub>a</sub> of two carboxylic acid groups and NH<sup>+</sup> in III has been determined to be 2.62, 5.59, and 10.1. PA III, evaluated as a potential antiscalant in reverse osmosis plants, at the concentrations of 5 and 20 ppm, imparted ≈100% efficiency for CaSO<sub>4</sub> scale inhibition from its supersaturated solution for over 50 and 500 min, respectively, at 40 °C. The synthesis of PA III in excellent yields from cheap starting materials and its very impressive performance may grant PA III a prestigious place as an environment-friendly phosphate-free antiscalant.

Received 21st October 2018  
 Accepted 13th November 2018

DOI: 10.1039/c8ra08723g

[rsc.li/rsc-advances](http://rsc.li/rsc-advances)

## 1. Introduction

Butler's cyclopolymerization protocol<sup>1</sup> has etched a place of distinction in the synthesis of polymers of tremendous technological importance.<sup>2–4</sup> Free radical-initiated polymerization of diallylammonium salts **A** led to **B** having pyrrolidine rings embedded into the macromolecules (Scheme 1). The macromolecule **B** represents the eighth most important architecture among synthetic high polymers.<sup>5,6</sup> Polydiallyldimethylammonium chloride **B** (R<sup>1</sup>=R<sup>2</sup>=Me), alone accounting for over 1000 patents and publications, has been produced to the tune of millions of pounds for a variety of industrial applications including water treatment.<sup>1</sup> Sulfur dioxide has been extensively used to synthesize alternate cyclopolymers **C** having numerous applications.<sup>7–9</sup> The reactivity ratios of amine (salt) (*r*<sub>A</sub>) and *r*<sub>SO<sub>2</sub></sub> being zero led to the alternation in **C**. Likewise, the almost zero reactivity ratios of *r*<sub>A</sub> and maleic acid (MA) (*r*<sub>MA</sub>) led to the exclusive formation of alternate copolymer **D** from alkylallyldiallylamine/MA ion pair **A**.<sup>10,11</sup> Interestingly, diallyldimethylammonium chloride (A)–MA–SO<sub>2</sub> is reported in

several patents<sup>12–14</sup> to give terpolymers in respective ratios of 50 : 25 : 25 (ref. 12) and 70 : 25 : 5.<sup>14</sup> However, the patents do not describe any micro-structural analysis. To our knowledge, no journal article has appeared to date to describe such terpolymerization involving A–maleic acid–SO<sub>2</sub> to give **E** (Scheme 1).

Amino-carboxylate and -phosphonate are important antiscalant and metal chelation motifs; as such, the decoration of repeating units with a high density of these potent functional groups is expected to impart, for instance, an antiscalant behavior. Looking at the zero reactivity ratios for both the monomer pairs: *r*<sub>A</sub> ≈ *r*<sub>SO<sub>2</sub></sub> ≈ 0 and *r*<sub>A</sub> ≈ *r*<sub>MA</sub> ≈ 0 (Scheme 1), we do fancy the success of the terpolymerization to pave the way to a great many interesting terpolymers **E**. Herein, we report a systematic study involving the cyclopolymerization of **A**, A–SO<sub>2</sub>, A–MA, and A–MA–SO<sub>2</sub> to investigate the course of action of an amine terminal radical –A\* whether it adds exclusively or preferentially onto SO<sub>2</sub> or MA or both.

## 2. Experimental section

### 2.1 Materials

Paraformaldehyde was purchased from Fluka Chemie AG. Diallylamine from Merck Schuchardt OHG, ammonium persulfate (APS), azobisisobutyronitrile (AIBN) and maleic acid from Sigma-Aldrich were used as received. Diallyldimethylammonium

Chemistry Department, King Fahd University of Petroleum & Minerals, Dhahran 31261, Saudi Arabia. E-mail: [shaikh@kfupm.edu.sa](mailto:shaikh@kfupm.edu.sa); Web: <http://faculty.kfupm.edu.sa/CHEM/shaikh/>; Fax: +966 13 860 4277; Tel: +966 13 860 3830

† Electronic supplementary information (ESI) available. See DOI: 10.1039/c8ra08723g





### 2.3 Synthesis of methyldiallylamine (7) and its hydrochloride salt 8

The procedure for the methylation of amines is adapted from the literature.<sup>18</sup> Formic acid (35 g, 85%, 0.646 mol) was added slowly (30 min) onto an ice-cold diallylamine (**1**) (49 g, 0.506 mol) in a 1 L RB flask under stirring. Paraformaldehyde (18.3 g, 0.613 mol) and water (33 mL) were added to the flask. The mixture in the flask, fitted with a long condenser, was stirred at 75–77 °C during which CO<sub>2</sub> evolution happened (30 min). Thereafter, the reaction mixture was heated to 90 °C; after the gas evolution stopped (15 min), the reaction mixture was cooled and saturated with the addition of a solution of NaOH (30 g, 0.75 mol) in water (30 mL). The separated organic layer of amine **7** was dried over NaOH and distilled at 107 °C (lit.<sup>19</sup> bp 109 °C) to obtain **7** as a colorless liquid (49 g, 87%).

A dry HCl gas was passed to a solution of methyldiallylamine (**7**) (25 g, 0.225 mol) in ether (150 mL) at 0 °C. Immediate precipitation of white salt **8** occurred. The passage of HCl was continued until the supernatant liquid becomes clear instead of cloudy. After filtration, the white salt was dried under vacuum to obtain **8** (30 g, 90%).  $\delta_{\text{H}}$  (D<sub>2</sub>O) 2.70 (3H, s), 3.65 (4H, d, *J* 7.3 Hz), 5.50 (4H, m), 5.82 (2H, m);  $\delta_{\text{C}}$  (D<sub>2</sub>O) 39.57 (1C, Me), 58.30 (2C, NCH<sub>2</sub>), 126.60 (2C, =CH), 127.33 (2C, =CH<sub>2</sub>). The <sup>13</sup>C spectral assignments was supported by DEPT 135 NMR analysis.

### 2.4 Polymer syntheses

**2.4.1 Procedure for 1 or 5/2/SO<sub>2</sub> terpolymerization.** Table 1 describes the polymerizations conditions (Scheme 1). For experiment under entry 1, SO<sub>2</sub> (705 mg, 11 mmol) was absorbed in a solution of monomer **1a** (1.38 g, 5.0 mmol) and MA **2** (0.70 g, 6.0 mmol) in DMSO (2.6 g) in an RB flask (10 mL). After purging the mixture with N<sub>2</sub>, initiator APS (0.260 g) was added to the stirring mixture in the closed flask at 21 °C for 24 h. The polymer mixture was dialyzed against 0.2 M HCl for 24 h with frequent change of 0.2 M HCl. Finally, the polymer solution was dialyzed against

distilled water for 6 h. The dialyzed solution was acidified with concentrated HCl (1.0 mL) and freeze-dried to obtain **4a**. Note that the acidification was intended to keep the nitrogens and carboxyls protonated. The FTIR and NMR spectra of the polymers resembled with the spectra of **1a**·HCl/SO<sub>2</sub> and **1b**·HCl/SO<sub>2</sub> copolymers **4a**<sup>20</sup> and **4b**<sup>21</sup> ( $y \approx 0$ ), respectively.

For the polymerization involving monomer **5**,<sup>17</sup> the crude reaction mixture was dialyzed against 2 M HCl followed by deionized water. Polymer **6** ( $y \approx 0$ ), precipitated out during dialysis, was dried under vacuum. The spectral analysis revealed the identical nature of the material **6** ( $y = 0$ ) described elsewhere.<sup>20</sup>

**2.4.2 Free radical polymerization of monomer 8.** A solution of salt **8** (8.86 g, 60 mmol) in water (3.5 g) and concentrated HCl (36 wt%) (0.5 g) in an RB flask (50 mL) fitted with a condenser was degassed with N<sub>2</sub> and then heated to 100 °C. APS was added in three portions (3 × 250 mg) with intervals of 3 min (Scheme 2). The temperature of the exothermic polymerization rose to 110 °C. The reaction mixture was continued to stir at the oil bath temperature of 100 °C for an additional 30 min. The product mixture was then dialyzed against distilled water and freeze-dried to obtain polymer **9** (7.7 g, 87%) as a white powder. (Found: C 56.7; H 9.58; N 9.4%. C<sub>7</sub>H<sub>14</sub>ClN requires C 56.94; H 9.56; N 9.49%;  $\nu_{\text{max}}$  (KBr): 3500 (broad), 2946, 2724, 1649 (H<sub>2</sub>O bending), 1461, 1107, 1053, 973, 909, 628, and 483 cm<sup>-1</sup>.  $[\eta]$  0.0805 dL g<sup>-1</sup> at 30 °C in 0.1 M NaCl.

**2.4.3 Photochemically initiated polymerization of monomer 8.** A sample of monomer **8** (200 mg, 1.4 mmol) in a vial was exposed to UV radiation at room temperature for 4 days. No polymerization occurred as indicated by <sup>1</sup>H NMR spectrum. Likewise, a solution of monomer **8** (295 mg, 2.0 mmol) in water (120 mg) was exposed to UV radiation at room temperature for 4 days giving **9** only in 5% yield as revealed by <sup>1</sup>H NMR spectrum. The yield was improved to 7.6% after further irradiation for 2 days.

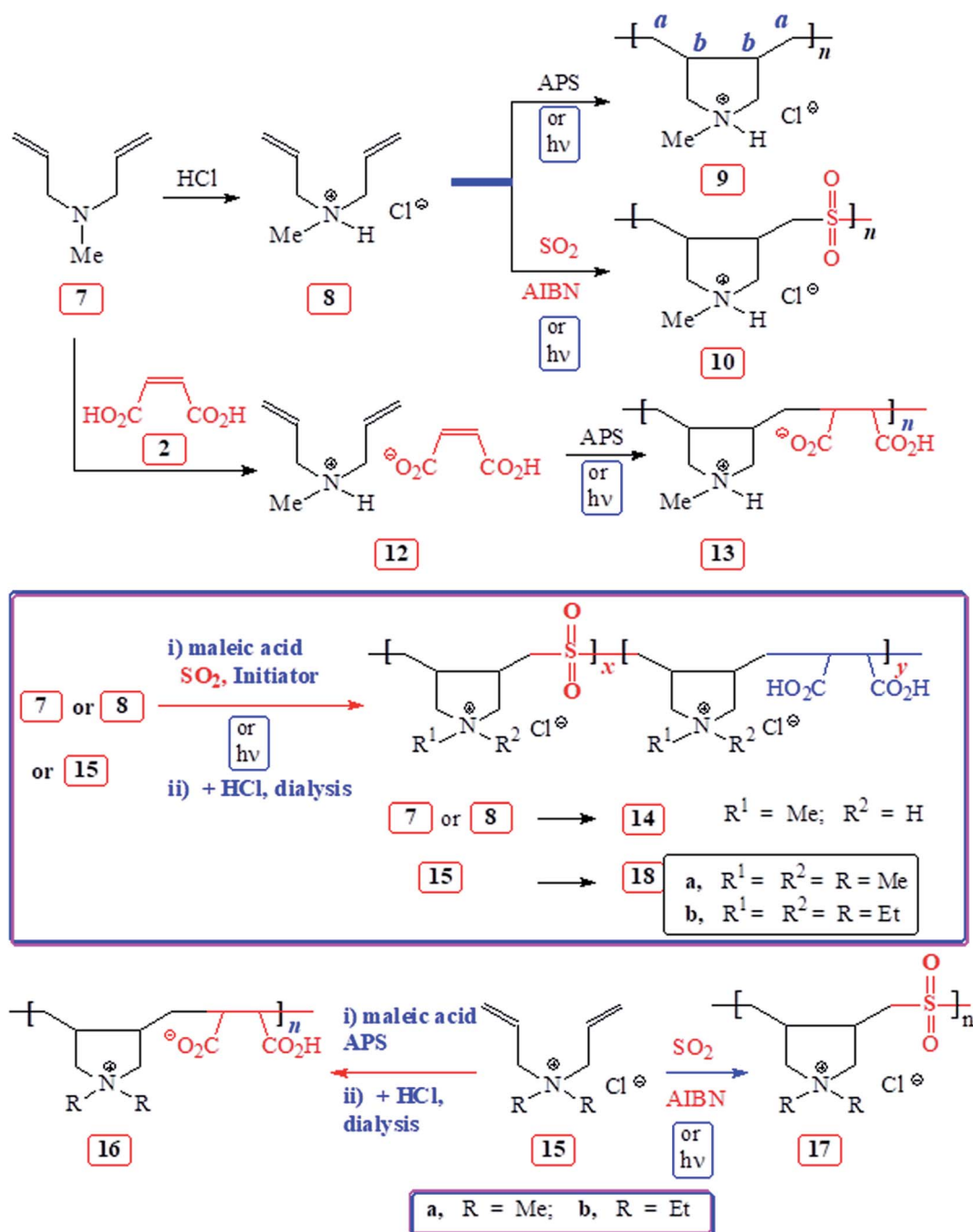
**2.4.4 Copolymerization of 8 with SO<sub>2</sub>.** To a solution of monomer **8** (5.02 g, 34 mmol) in DMSO (8.4 g) was absorbed SO<sub>2</sub>

Table 1 Attempted cycloterpolymerization<sup>a</sup> of monomers **1a**, **1b** and **5** with maleic acid **2** and SO<sub>2</sub>

Entry	Amine <b>1</b> (mmol)	MA <b>2</b> (mmol)	SO <sub>2</sub> mmol	Initiator <sup>c</sup> (mg)	Temp.	Yield <sup>b</sup>	$[\eta]$ <sup>c</sup> (dL g <sup>-1</sup> )
1	<b>1a</b> : 5	6	11	APS (260)	21	<b>4a</b> : 39 (67)	0.0721
2	<b>1a</b> : 5	6	11	APS (70)	45	<b>4a</b> : 34 (68)	0.0562
3	<b>1a</b> : 5	6	11	APS (260)	45	<b>4a</b> : 48 (86)	0.0571
4	<b>1a</b> : 5	10	16	APS (260)	45	<b>4a</b> : 62 (90)	0.0462
5	<b>1a</b> : 5	6	11	APS (96)	65	<b>4a</b> : 11 (72)	0.0401
6	<b>1a</b> : 5	6	11	APS (210)	65	<b>4a</b> : 53 (60)	0.0454
7	<b>1a</b> : 5	6	11	APS (250)	65	<b>4a</b> : 48 (81)	0.0228
8	<b>1a</b> : 5	6	11	AIBN (46)	65	<b>4a</b> : trace (28)	—
9	<b>1a</b> : 5	6	11	AIBN (100)	65	<b>4a</b> : 27 (60)	0.0211
10	<b>1b</b> : 5	6	11	APS (140)	65	<b>4b</b> : 49 (72)	0.0355
11	<b>5</b> : 5	6	11	APS (200)	65	<b>6</b> : 61 (67)	0.532
12	<b>5</b> : 5	6	11	AIBN (50)	65	<b>6</b> : 67 (71)	0.519
13	—	6	5	APS (140)	45	No polymer	—
14	—	6	5	TBHP (100)	Temp. <sup>d</sup>	No polymer	—

<sup>a</sup> Copolymerization reactions were carried out in DMSO (2.6 g) in the presence of ammonium persulfate (APS) or azoisobutyronitrile (AIBN) or *tert*-butylhydroperoxide for 48 h. <sup>b</sup> Polymer obtained is written in bold followed by isolated yields; the percent conversion determined by <sup>1</sup>H NMR analyses of the crude reaction mixture are written in parentheses. <sup>c</sup> Viscosity of 1–0.25% polymer solution in 0.1 M NaCl at 30 °C was measured with Ubbelohde viscometer ( $K = 0.005317 \text{ mm}^2 \text{ s}^{-2}$ ). <sup>d</sup> At –10 °C for 2 days, then at 0 and 25 °C for 2 days each.





Scheme 2 Synthesis of homopolymer from **8**, alternate copolymers from **7/MA**, **15/MA**, **8/SO<sub>2</sub>**, **15/SO<sub>2</sub>**, and terpolymers from **7 or 8/MA/SO<sub>2</sub>** and **15/MA/SO<sub>2</sub>**.

(2.18 g, 34 mmol). After adding initiator AIBN (200 mg), the reaction mixture was heated at 65 °C inside a closed vessel for 24 h. The resultant polymer mixture was dialyzed against distilled water. The dialyzed solution was treated with 2.0 g concentrated HCl (37%, 20 mmol) and then freeze-dried to obtain a white powder of copolymer **10** (6.7 g, 93%).  $[\eta]$  0.276 dL g<sup>-1</sup> at 30 °C in 0.1 M NaCl. (Found: C 39.4; H 6.8; N 6.5%. C<sub>7</sub>H<sub>14</sub>ClNO<sub>2</sub>S requires C 39.71; H, 6.67; N 6.62%);  $\nu_{\text{max}}$  (KBr): 3452 (broad), 2955, 2719, 1636 (H<sub>2</sub>O bending), 1466, 1413, 1304, 1128, 1036, 963, 856, 773, and 517 cm<sup>-1</sup>.

**2.4.5 Methylallylamine (7) and maleic acid (2) ion pair 12.** Maleic acid **2** (1.16 g, 10.0 mmol) was added to a biphasic mixture of amine **7** (1.11 g, 10.0 mmol) in water (8 mL) and stirred at 25 °C for 30 min. Exothermic neutralization led to a homogeneous solution which was freeze-dried to obtain ion pair **12** as a colorless liquid in quantitative yield.  $\nu_{\text{max}}$  (neat): 3496 (strong), 3375 (strong and broad), 3031, 2962, 2656 (R<sub>3</sub>NH<sup>+</sup>), 2516 (R<sub>3</sub>NH<sup>+</sup>), 2356 (R<sub>3</sub>NH<sup>+</sup>), 1704, 1623, 1581, 1477, 1363, 1202, 1082, 988, 869, 710, 653, and 568 cm<sup>-1</sup>.  $\delta_{\text{H}}$  (D<sub>2</sub>O) 2.55 (3H, s), 3.43 (2H, ABX, *J* 7.5, 13.4 Hz), 3.57 (2H, ABX, *J* 7.0, 13.4



(Hz), 5.35 (4H, m), 5.67 (2H, m), 6.08 (2H, s);  $\delta_{\text{C}}$  ( $\text{D}_2\text{O}$ ) 39.37 (1C, Me), 58.07 (2C,  $\text{NCH}_2$ ), 126.37 (2C,  $=\text{CH}$ ), 127.19 (2C,  $=\text{CH}_2$ ), 135.09 (CH= $\text{CH}$ ), 171.14 (C=O). The  $^{13}\text{C}$  spectral assignments were supported by DEPT 135 NMR.

**2.4.6 Copolymerization of 7 and MA 2.** In an RB flask fitted with a condenser, were taken amine 7 (2.22 g, 20.0 mmol), MA 2 (2.54 g, 22.0 mmol) and water (2.04 g). The homogeneous mixture was stirred at 100 °C under  $\text{N}_2$ , and initiator APS was added (2 × 200 mg) onto the mixture over 4 min. The exothermic polymerization started, and the mixture was stirred at 100 °C (10 min), cooled, dialyzed against deionized water, and freeze-dried to obtain a white powder of alternate poly-ampholyte (PA) 13 (3.68 g, 81%). The crude mixture revealed the monomer conversion of 86% as indicated by  $^1\text{H}$  NMR spectrum. (Found: C 57.8; H 7.7; N 6.0%.  $\text{C}_{11}\text{H}_{17}\text{NO}_4$  requires C 58.14; H 7.54; N 6.16%).  $\nu_{\text{max}}$  (KBr): 3455 (broad), 2949, 2729, 2357, 1714, 1635, 1574, 1464, 1391, 1207, 1053, 810, 661 and 566  $\text{cm}^{-1}$ .

**2.4.7 Procedure for 7 or 8/ $\text{SO}_2$  terpolymerization.** Table 2 describes the polymerizations conditions. The polymerizations were carried out as described under Section 2.4.1. After completion of the polymerization, the crude mixture was dialyzed against 0.2 M HCl with frequent change of the 0.2 M HCl for a duration of 24 h, and finally, dialyzed against distilled water for 6 h. The resulting solution was acidified with concentrated HCl (1.0 mL) and freeze-dried to obtain polymer 14. Note that the acidification was carried out to keep the nitrogens and carboxyls protonated. The FTIR and NMR spectra of the polymer 14 resembled with the spectra of 7 HCl/ $\text{SO}_2$  copolymer 10, thereby implying the value of  $\gamma \approx 0$ .

**2.4.8 Procedure for 15/2/ $\text{SO}_2$  co- and terpolymerization.** Table 3 describes the polymerizations conditions (Scheme 2). The polymerizations of monomers 15 were carried out as described under Section 2.4.1. After the elapsed time, the reaction mixture (involving MA) was dialyzed against 0.5 M HCl for 24 h with frequent change of the 0.5 M HCl to remove excess MA, followed

by dialysis against distilled water for 6 h. The resulting solution freeze-dried to obtain polymer 16. However, the dialyzed solution of 18, after acidification with concentrated HCl (1.0 mL), was freeze-dried. (Acidification was carried out to keep the carboxyl groups protonated). In the case where MA was not involved, the polymer 17 was simply purified by dialysis against distilled water. The FTIR and NMR spectra of the polymer 18 resembled with the copolymer 17, thereby implying the value of  $\gamma \approx 0$ .

## 2.5 Determination of basicity constants by titrations

The basicity constant ( $K$ ) of the three basic centers in PA 13 were determined using reported procedures<sup>11,22</sup> and conditions described in Table S1.†  $\log K_{\text{is}}$  were calculated using the Henderson–Hasselbalch equation (eqn (2); Scheme 3).

## 2.6 Use of synthesized PA 13 as an antiscalant

The inhibition of  $\text{CaSO}_4$  scale formation from its supersaturated solution was examined in the presence of various concentrations of PA 13 in an aqueous solution containing  $\text{Ca}^{2+}$  (2600  $\text{mg L}^{-1}$ ) and  $\text{SO}_4^{2-}$  (6300  $\text{mg L}^{-1}$ ) at  $40 \pm 1$  °C as described.<sup>22</sup> The conductivity decreased suddenly after an induction time, owing to the formation of scale as confirmed by visual inspections.

# 3. Results and discussion

## 3.1 Polymer synthesis

The results of APS-initiated terpolymerization of monomers 1a or 1b or 5 with  $\text{SO}_2$  and MA 2 are given in Table 1 (Scheme 1). The attempted copolymerization of MA- $\text{SO}_2$  was unsuccessful (entries 13 and 14). Terpolymerization of 1a-MA- $\text{SO}_2$  was conducted under various conditions using APS or AIBN initiator. The polymer 4a was isolated after extensive dialysis against aqueous HCl to remove unreacted MA and replace the maleate anion with  $\text{Cl}^-$  ions. The spectral (NMR and IR) analysis

Table 2 Attempted cycloterpolymerization of monomer 7 or 8 with  $\text{SO}_2$  and maleic acid 2

Entry	7 or 8 (mmol)	MA 2 (mmol)	$\text{SO}_2$ (mmol)	DMSO (g)	Initiator (mg)	Temp (°C)	Time (h)	Yield <sup>a</sup>	$[\eta]^b$ ( $\text{dL g}^{-1}$ )
1 <sup>c</sup>	7: (5)	6	11	2.3	APS: 85	45	72	14: 21 (63)	0.141
2 <sup>c</sup>	7: (5)	6	11	2.3	APS: 150	45	72	14: 31 (57)	0.125
3	7: (5)	11	16	2.3	APS: 85	45	72	14: 23 (63)	0.121
4	7: (5)	11	16	2.3	APS: 175	45	48	14: 47 (60)	0.182
5	7: (5)	11	16	2.3	APS: 260	65	24	14: 32 (83)	0.129
6	7: (5)	22	31	2.8	APS: 260	65	24	14: 62 (85)	0.172
7 <sup>c</sup>	7: (5)	6	11	2.3	AIBN: 75	65	36	14: 0 (10)	—
8 <sup>d</sup>	8: (1)	10	25	4.6	APS: 360	45	48	14: 51 (67)	—
9 <sup>d</sup>	8: (5)	5	5	0	Dark	23	24	14: 0 (0)	—
10 <sup>d</sup>	7: (5)	5	6	0	UV	23	168	14: 26 (43)	0.278
11 <sup>e</sup>	8: (5)	5	10	0	UV	23	24	14: 45 (62)	0.329
12 <sup>e</sup>	8: (5)	5	10	0	UV	−15	4	14: 43 (67)	0.273
13 <sup>e</sup>	8: (5)	5	10	1.0	UV	23	24	14: 43 (83)	0.471
14	8: (5)	5	10	MeOH: 1.0	UV	−10	6	14: 15 (35)	0.192
15	8: (5)	0	4.5	0	UV	23	24	10: 54 (72)	0.836
16	8: (5)	0	0	$\text{H}_2\text{O}$ : 0.3	UV	23	144	9: — (7.6)	—

<sup>a</sup> Isolated yields is followed by the percent conversion written in parentheses. As determined by  $^1\text{H}$  NMR analyses of the crude reaction mixture.

<sup>b</sup> Viscosity of 1–0.25% polymer solution in 0.1 M NaCl at 30 °C was measured with Ubbelohde viscometer ( $K = 0.005317 \text{ mm}^2 \text{ s}^{-2}$ ). <sup>c</sup> Cloudy reaction mixture after 4 h. <sup>d</sup> MA remained partially soluble. <sup>e</sup> Solidified.



Table 3 Attempted cyclooligomerization of monomers **15** with SO<sub>2</sub> and maleic acid 2

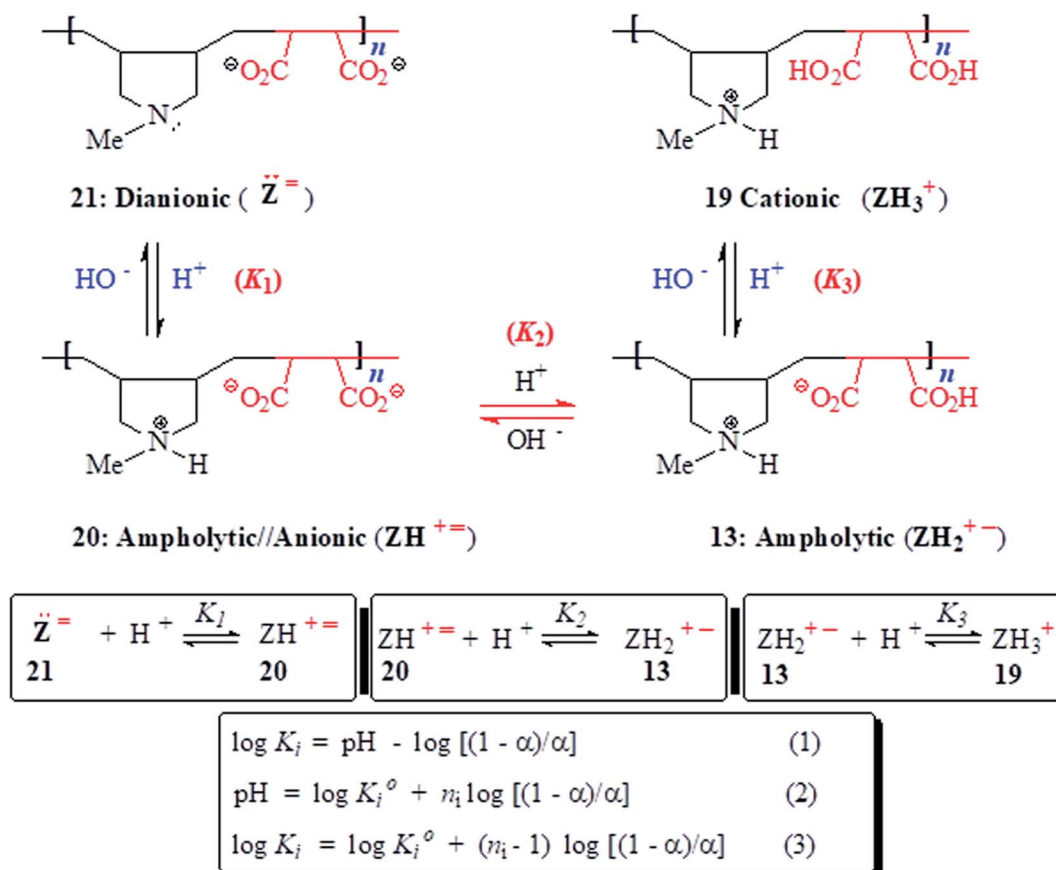
Entry	<b>15</b> (mmol)	MA 2 (mmol)	SO <sub>2</sub> (mmol)	DMSO (g)	Initiator (mg)	Temp (°C)	Time (h)	Yield (%)	[η] <sup>a</sup> (dL g <sup>-1</sup> )
1	<b>15a</b> : 5	6	—	H <sub>2</sub> O (1.0)	APS: 250	100	0.25	<b>16a</b> : 27 <sup>b</sup>	0.102
2 <sup>c</sup>	<b>15a</b> : 5	—	6	0	UV	23	48	<b>17a</b> : 80	1.86
3	<b>15a</b> : 5	6	11	3.0	APS: 215	55	24	<b>18a</b> : 87	0.317
4	<b>15a</b> : 5	6	6 <sup>d,e</sup>	0	UV	23	48	<b>18a</b> : 71	1.67
5	<b>15b</b> : 5	—	6	2.6	APS: 250	55	2	<b>17b</b> : 96	0.552
6	<b>15b</b> : 5	—	6	2.6	AIBN: 29	55	72	<b>17b</b> : 87	0.253
7	<b>15b</b> : 5	6	10	2.8	APS: 125	55	48	<b>18b</b> : 88	0.401

<sup>a</sup> Viscosity of 1–0.0625% polymer solution in 0.1 N NaCl at 30 °C was measured with Ubbelohde viscometer ( $K = 0.005317 \text{ mm}^2 \text{ s}^{-2}$ ). <sup>b</sup> 98% conversion as revealed by <sup>1</sup>H NMR of crude mixture. <sup>c</sup> White solid mixture in the beginning and no phase change throughout. <sup>d</sup> Not been able to add more SO<sub>2</sub>. <sup>e</sup> Slightly turbid in the beginning but hardened towards the end.

revealed that terpolymer **4a** resembled the **1a**-SO<sub>2</sub> copolymer **4a** ( $y = 0$ ),<sup>20</sup> except a minor <sup>13</sup>C C=O peak at  $\approx \delta$  180 ppm (*vide infra*) and a minor vibration at  $\approx 1728 \text{ cm}^{-1}$  attributed to C=O of CO<sub>2</sub>H in the IR spectrum. The absence of alkene carbons at  $\delta$  135 ppm excluded the presence of MA either as a free acid or the maleate ions; however, the presence of minor C=O signals suggests the incorporation of maleic acid into the polymer backbone. The MA does undergo propagation, but the addition is reversible as indicated by the presence of fumaric acid (FA) (*trans*-HO<sub>2</sub>CC=CHCO<sub>2</sub>H) in the unreacted reaction mixture, in addition to its original *cis*-counterpart MA in  $\alpha \approx 1 : 4$  ratio. The radical having MA terminal: R-CH(CO<sub>2</sub>H)-CH(CO<sub>2</sub>H)· may undergo quick reversion to give R· and MA as well as FA.

Likewise, **1b**-MA-SO<sub>2</sub> (entry 10) and **5**-MA-SO<sub>2</sub> (Table 1, entries 11 and 12) terpolymerizations afforded **4b** and **6**, respectively (Scheme 1), whose spectra are identical to those of **4b** ( $y = 0$ )<sup>21</sup> and **6** ( $y = 0$ ),<sup>20</sup> except that a very minor peak due to C=O in the <sup>13</sup>C NMR and IR spectra indicate the very minor incorporation of MA.

Monomer **8** was homo- and co-polymerized with SO<sub>2</sub> to obtain cationic polyelectrolytes **9** and **10** in excellent yields of 87 and 93%, respectively (see Experimental) (Scheme 2). Homopolymerization of **8** in an aqueous solution under UV light ( $\lambda = 365 \text{ nm}$ ) was very slow; after 6 days, it gave CPE **9** in a very low yield of 7.6% (entry 16, Table 2). The bulk photopolymerization **8**-SO<sub>2</sub> (entry 15, Table 2) in the absence of

Scheme 3 pH Induced changes in the charge types in the backbone of **13**, **19**–**21**.

solvent gave CPE **10** having much higher intrinsic viscosity  $[\eta]$  of  $0.836 \text{ dL g}^{-1}$  than that of the thermally initiated copolymer with a  $[\eta]$  of  $0.276 \text{ dL g}^{-1}$  (Experimental section 2.4.4).

Terpolymerization of **7** or **8-MA-SO<sub>2</sub>** was extensively studied using free radical initiators APS, AIBN or UV radiation at  $\lambda$  365 nm (Scheme 2). The results are included in Table 2. Note that the isolated yields after dialysis are low as compared to the NMR conversion since the low molecular weight polymer fractions leave the dialysis bag. The <sup>1</sup>H and <sup>13</sup>C NMR spectra of the samples from entries 1–14 dealing with the **7** or **8-MA-SO<sub>2</sub>** terpolymerizations afforded **14**, which is almost identical to the **8-SO<sub>2</sub>** copolymer **10** except the IR has very minor C=O vibrational peak at  $\approx 1728 \text{ cm}^{-1}$  indicating the presence of MA repeating units in **14**. A series of IR spectra of copolymer **10** containing 0–5 mol% succinic acid (CH<sub>2</sub>)<sub>2</sub>(CO<sub>2</sub>H)<sub>2</sub> helped us to estimate the proportion of MA unit in **14** as  $\approx 1$ –3 mol%. The strong non-overlapping IR vibrations of SO<sub>2</sub> unit in **10** at 1304 and 1128 cm<sup>-1</sup> and the C=O vibration of CO<sub>2</sub>H at  $\approx 1728 \text{ cm}^{-1}$  were used to estimate the MA mol%.

Next, we focussed our attention to the polymerization of quaternary ammonium salts **15** as outlined in Scheme 2; the polymerization conditions and the results are included in Table 3. The **15a-MA** copolymerization afforded **16a** in 27% isolated yields, while the crude mixture before dialysis indicated 98% conversion as calculated from <sup>1</sup>H NMR spectrum (entry 1). The spectral data matched with that reported for the polymer.<sup>23</sup> Bulk copolymerization of **15a-SO<sub>2</sub>** under UV light<sup>24</sup> afforded copolymer **17a** in excellent yield (entry 2). The very high  $[\eta]$  value of  $1.86 \text{ dL g}^{-1}$  indicated the high molar mass of the polymer. The thermal **15b-SO<sub>2</sub>** (ref. 19) copolymerization afforded copolymer **17b** also in excellent yields (entries 5 and 6). The IR and NMR spectra of **17a, b** matched with the reported data.<sup>25,26</sup> The terpolymerizations: **15a-MA-SO<sub>2</sub>** (entries 3 and 4) and **15b-MA-SO<sub>2</sub>** (entry 7) gave polymers **18a** and **18b**, respectively; their NMR and IR spectra matched with those of the respective copolymers **17a** and **17b** except the minor C=O vibration at  $\approx 1728 \text{ cm}^{-1}$  indicating the incorporation of  $\approx 1$ –3 mol% MA.

All the reactivity ratios in the pairs: amine salt–MA and amine salt–SO<sub>2</sub> are almost zero (*vide supra*) thereby implying that under the reaction conditions, amine salt or MA or SO<sub>2</sub> cannot undergo homopolymerization, instead they must give alternate copolymers as experimentally observed. MA–SO<sub>2</sub> reaction has been shown to give neither homo- nor co-polymer (entries 13 and 14, Table 1). In the numerous amine salt–MA–SO<sub>2</sub> terpolymerizations, the extent of MA incorporation is only 1–2 mol%. In every instance, amine salt–SO<sub>2</sub> copolymer was obtained and no trace of amine salt–MA copolymer could be identified. The claim in the patented literatures<sup>12–14</sup> that the formation of terpolymer: diallyldimethylammonium chloride–maleic acid–SO<sub>2</sub> having repeating unit composition of 50 : 25 : 25 and 70 : 25 : 5 are doubtful. A composition ratio of 50 : 25 : 25 may indeed be a result of a mixture of two alternate copolymers of diallyldimethylammonium chloride–maleic acid and diallyldimethylammonium chloride–SO<sub>2</sub>. The current work confirms that the amine salt–MA–SO<sub>2</sub> cannot be terpolymerized to any meaningful extent.

### 3.2 Solubility behavior

Cationic polymers **4a, b** ( $y \approx 0$ ), **9, 10** and **14** ( $y \approx 0$ ) are water-soluble, while the PZ **6** ( $y \approx 0$ ) is insoluble in water but soluble in 0.8 M HCl.<sup>20</sup> The water-solubility of **13**, unlike most electro-neutral polymers,<sup>27–29</sup> could be attributed to the less effective participation of the crowded CO<sub>2</sub><sup>-</sup> to undergo electrostatic associations with NH<sup>+</sup> for manifestation of ampholytic interactions.<sup>2</sup> Moreover, the hydrophilicity and solubility of the ampholytic motifs increase as a result of the increased dipole moment ( $\mu$ ) because of the large separation between NH<sup>+</sup> and CO<sub>2</sub><sup>-</sup>.<sup>30,31</sup>

### 3.3 Spectroscopic characterization

The strong IR bands at 1304 and 1128 cm<sup>-1</sup> were assigned to the vibrations of SO<sub>2</sub> unit in **10**. The absorption band at  $\approx 1714$  and 1574 cm<sup>-1</sup> is attributed to the C=O stretch of CO<sub>2</sub>H and CO<sub>2</sub><sup>-</sup> in (+<sup>-</sup>) **13**.<sup>32</sup>

The NMR spectra of several polymers are displayed in Fig. 1 and 2. For the monomer pair **12**, alkene protons of the diallyl amine part and maleate motif appeared at  $\delta$  5.5–6 ppm and 6.08 ppm, respectively (Fig. 1a), while the corresponding carbons are displayed at  $\delta$  126.4 (=CH), 127.2 (2C, =CH<sub>2</sub>), and 135.1 (CH=CH) (Fig. 2a). The low molar masses (as suggested by low viscosity values) and the absence of spectral signal for residual alkene protons or carbons of the polymers **9, 10** and **13** are indicative of degradative chain transfer<sup>33</sup> involving allylic hydrogens or a termination reaction by coupling.<sup>34</sup> The compact coil<sup>10</sup> conformation of MA-copolymer (+<sup>-</sup>) **13** is reflected in the broadened <sup>1</sup>H as well as <sup>13</sup>C NMR spectra (Fig. 1d and 2d), whereas the spectral signals are found to be sharp for homopolymer **9** or SO<sub>2</sub>-copolymer **10** (Scheme 2) (Fig. 1b or 1c). The incorporation of MA in (+<sup>-</sup>) **13** is confirmed by the presence of a broad signal around  $\delta$  180 ppm (Fig. 2d). Elemental analysis and the spectral data confirmed the formation of the alternate copolymer because both the reactivity ratios  $r_{\text{amine}}$  and  $r_{\text{MA}}$ , are expected to be close to zero.<sup>10,11</sup> Integration of the relevant carbon signals<sup>35,36</sup> revealed a 3 : 1 *cis/trans* ratio of the ring substituents at C<sub>b,b</sub> (Scheme 2).

### 3.4 TGA and viscosity behaviors PA (+<sup>-</sup>) **13**

TGA plot for a PA **13** (dried under vacuum at 55 °C for 6 h) revealed the weight losses at various temperature ranges (Fig. 3a). The presence of adjacent CO<sub>2</sub>H groups would lead to the formation of anhydride motifs with the loss of water as reflected by an 8.3% weight loss up to 200 °C. In fact, a loss of 1 molecule of water per repeating unit is calculated to be 7.9%. In the 200–380 °C range, maleic anhydride is itself released from the polymer backbone thereby accounting for the loss of  $\approx 41.2\%$  as compared to a calculated value of 46.9%.<sup>10,37</sup> A 48% loss in the 380–800 °C range is attributed to the removal of the amine units.

The viscosities of PA (+<sup>-</sup>) **13** are presented in Fig. 3b. The increase in viscosity with the increasing salt concentrations demonstrates the antipolyelectrolytic<sup>38</sup> nature of the poly-ampholyte [*cf.* Fig. 3b(i–iv)]. The ampholytic dipole is not perfectly electroneutral, rather has a residual negative charge on CO<sub>2</sub><sup>-</sup> since Na<sup>+</sup> cannot effectively neutralize it as compared to the greater



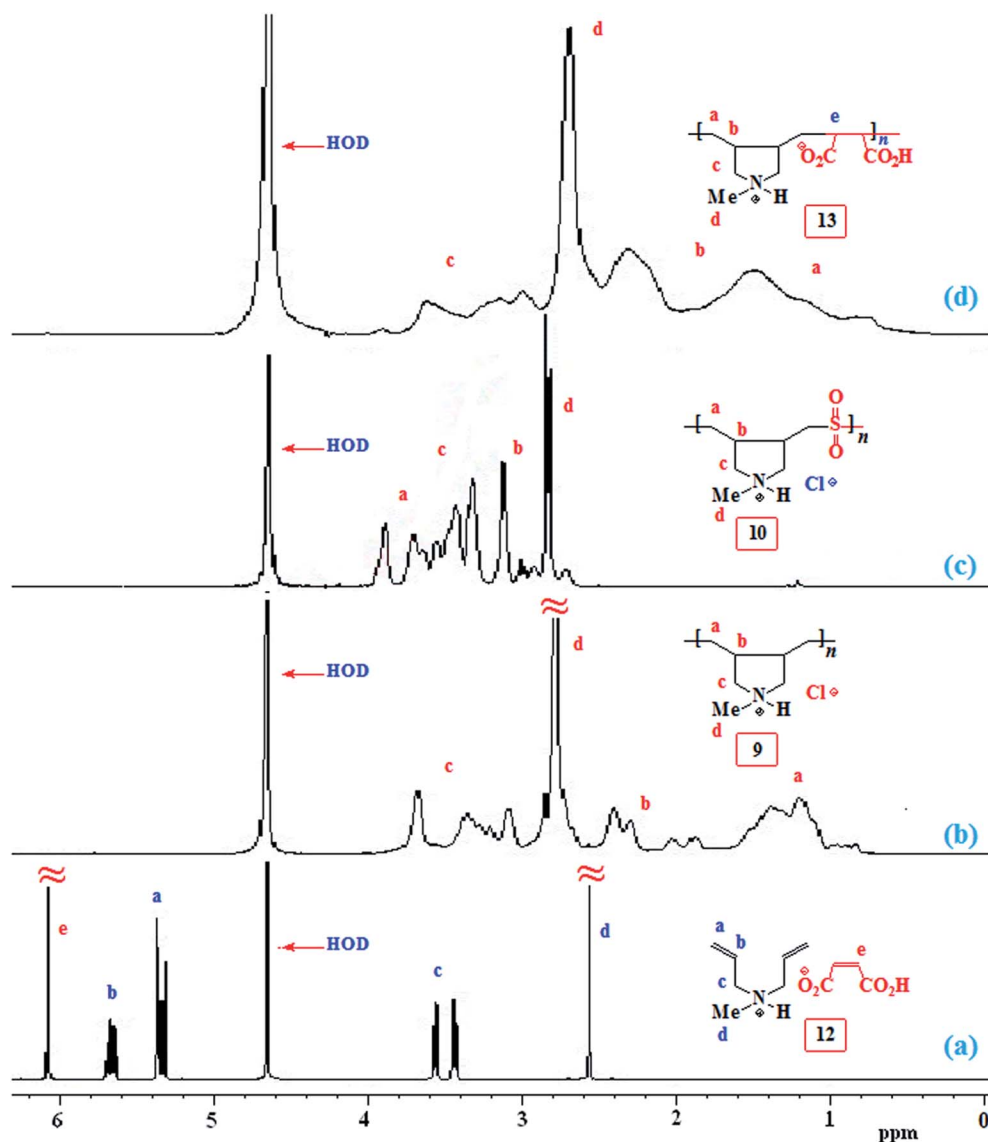


Fig. 1  $^1\text{H}$  NMR spectrum of (a) 12, (b) 9, (c) 10, and (d) 13 in  $\text{D}_2\text{O}$ .

shielding of  $\text{N}^+$  by  $\text{Cl}^-$ .<sup>39–41</sup> The magnitude of the excess negative charge, hence the viscosity, increases with salt concentrations.

PA ( $+^-$ ) 13 becomes a cationic polyelectrolyte 19 by protonation of  $\text{CO}_2^-$  and as such its viscosity becomes higher in 0.1 M HCl because of repulsion among positive charges (Fig. 3b-v) (Scheme 3). The neutralization of 13 with one or two equivalents of NaOH leads to polyampholyte/anion ( $+^{\ominus}$ ) 20 and polydianion ( $\ominus\ominus$ ) 21, the greater charge imbalance in the latter makes it more viscous (Fig. 3b-vi and vii).

Strong interactions of materials of GPC columns with functional groups like amine and  $\text{CO}_2^-$  prevented the determination of molar masses of the polymers like 13. Similar observation was reported earlier.<sup>10</sup> Purification by extensive dialysis with membrane of MWCO of 6000–8000 daltons indicates the products as true polymers not oligomers. The use of higher initiator dose along with degradative chain transfer termination process<sup>33</sup> led to PA 13, having low molar mass as indicated by its lower  $[\eta]$  value.

The intrinsic viscosities of the synthesized polymers 4a, 4b, 6, 9, 10, 13, 14, 16–18 are reported in the Tables 1–3. Since the MA incorporation is very minimal, 4a, 4b and 6 with the value of  $y \approx 0$  resembled the copolymers 4a, 4b and 6 ( $y = 0$ ) whose molar mass and  $[\eta]$  are amply described.<sup>20,21</sup> Similarly, polymers 17a, b which are similar to 18a, b ( $y \approx 0$ )<sup>23,25,26</sup> and 16a<sup>32</sup> have been extensively characterized in terms of viscosity and molar mass.

### 3.5 Basicity constant

As outlined in Scheme 3, the protonation constant  $K$  of three basic centers ( $\ominus\ominus$ ) 21 are calculated using eqn (3) where  $\log K^\circ = \text{pH}$  at  $\alpha$  (degree of protonation) = 0.5. The variation from the true basicity constant depends on the value of  $n$  which equals 1 for small molecules. The values of ' $n$ ' and  $\log K^\circ$  were extracted from the slope and intercept of the  $\text{pH}$  vs.  $\log[(1 - \alpha)/\alpha]$  straight-line plot. The respective  $\log K_1^\circ$ ,  $\log K_2^\circ$  and  $\log K_3^\circ$  were



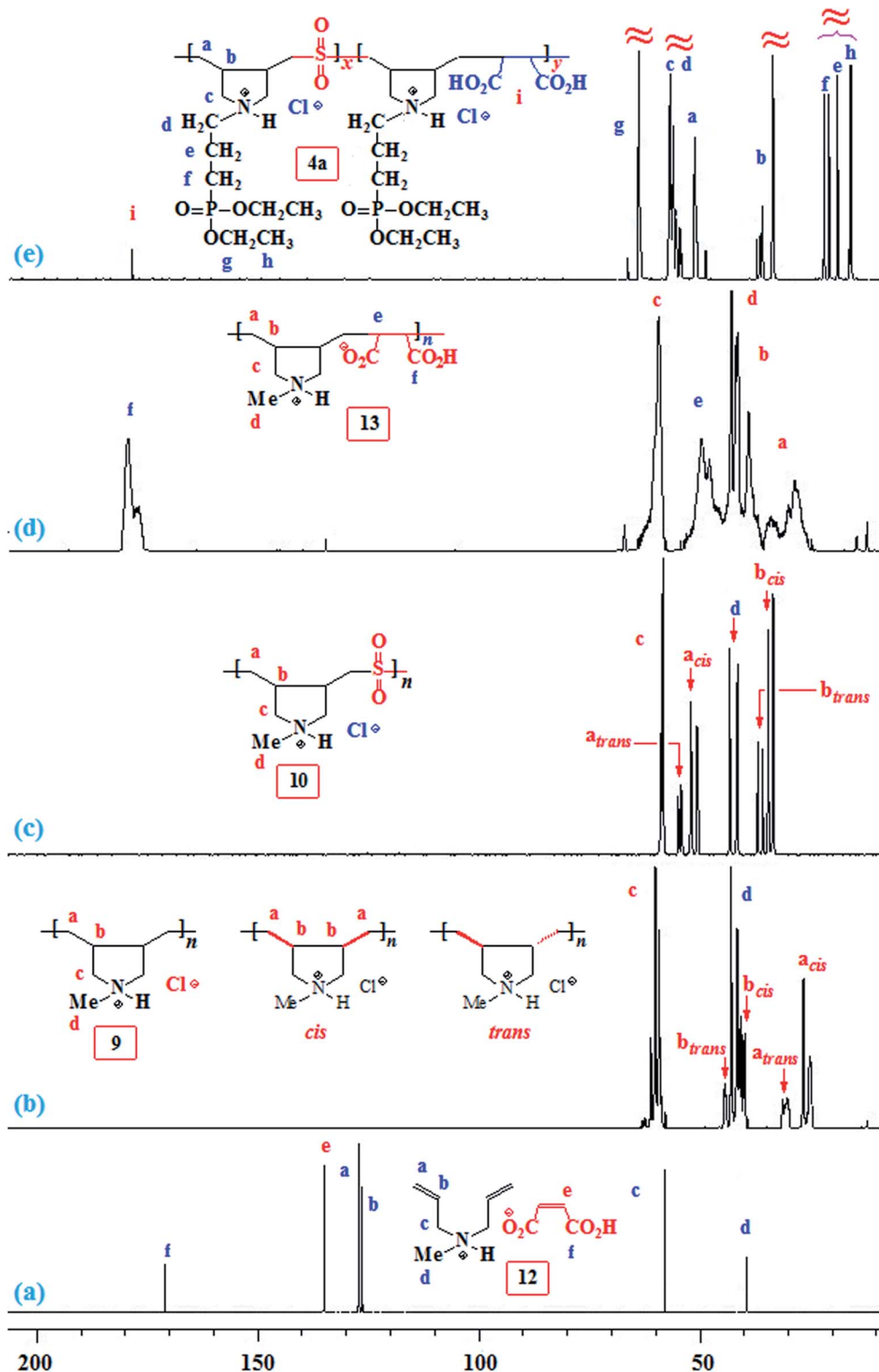


Fig. 2  $^{13}\text{C}$  NMR spectrum of (a) 12, (b) 9, (c) 10, (d) 13, and (e) 4a in  $\text{D}_2\text{O}$ .

determined to be 10.1, 5.59 and 2.62, with the corresponding  $n_1$ ,  $n_2$  and  $n_3$  values of 1.15, 2.19 and 0.48 (Table S1†).

All the  $n$  values, especially  $n_2$  and  $n_3$ , are reflective of the “apparent”<sup>42,43</sup> nature of the  $K_i$ s which changes with the  $\alpha$  as shown in Fig. 3c. The  $n$  value reflects a measure of the poly-electrolyte index. There are significant decrease and increase of

$\log K_2$  and  $\log K_3$ , respectively, with increasing  $\alpha$ , while the  $\log K_1$  remains almost constant since the associated  $n$  value of 1.15 is not far from 1.

With increasing  $\alpha$ , the equilibrium:  $[(\text{ZH}^{+\ominus}) \text{ 20} + \text{H}^+ \rightleftharpoons (\text{ZH}_2^{+\oplus}) \text{ 13}]$  is shifted to the right thereby decreasing  $\log K_2$  as a consequence of decreasing negative charge density that



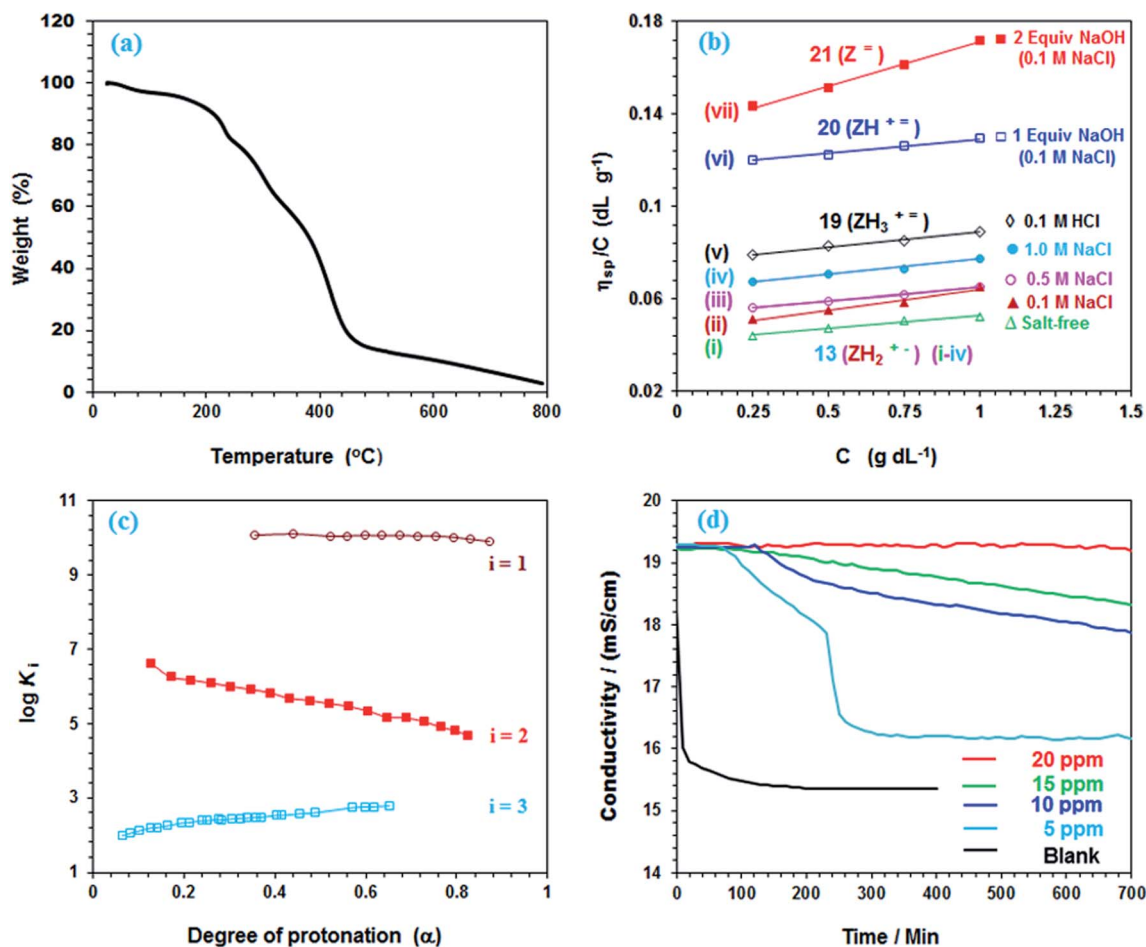


Fig. 3 (a) TGA curves of **13**; (b) the viscosity behavior at 30 °C of polyampholyte **13** (i)  $\Delta$  in salt-free water, (ii)  $\blacktriangle$  in 0.1 M NaCl, (iii)  $\circ$  in 0.5 M NaCl, (iv)  $\bullet$  in 1.0 M NaCl, (v)  $\diamond$  in 0.1 M HCl, and (vi)  $\square$  in the presence of 1 equiv. NaOH in 0.1 M NaCl, and (vii)  $\blacksquare$  in the presence of 2 equiv. NaOH in 0.1 M NaCl; (c) plot for the apparent  $\log K_i$  versus degree of protonation ( $\alpha$ ) in salt-free water  $\square$  ( $\log K_3$ , run 2, Table S1†),  $\blacksquare$  ( $\log K_2$ , run 2, Table S1†) and  $\circ$  ( $\log K_3$ , run 2, Table S1†); (d) conductivity of a supersaturated solution of  $\text{CaSO}_4$  in the presence (5, 10, 15, 20 ppm) of **13** and in the absence (blank) of antiscalant.

encourages protonation. This is in contrast to the increase of  $\log K_3^\circ$  [involving  $(\text{ZH}_2^{+-})$  **13** +  $\text{H}^+$   $\rightleftharpoons$   $(\text{ZH}_3^{++})$  **19**], whereby protonation of a repeating unit also decreases the overall negative charges of the polymer chain. The  $n$  values  $>$  or  $<$  1 are caused by entropy effects.<sup>42,44</sup> With each protonation, a repeating unit (RU) in ampholytic/anionic  $(\text{ZH}^{+-})$  **20** collapses into an ampholytic RU of  $(\text{ZH}_2^{+-})$  **13**. Ampholytic/anionic  $(\text{ZH}^{+-})$  **20** having excess negative charges is more hydrated than PA  $(+^-)$  **13** as supported by the higher viscosity value of the former (*cf.* Fig. 3b-vi vs. 3b-ii). The protonation of a RU leads to an entropically favourable release of water of hydration. For  $(\text{ZH}^{+-})$  **20**, as the  $\alpha$  increases, the average number of water molecules per RU in a polymer chain decreases which leads to a decrease in the magnitude of the positive entropy changes. Since the exothermic  $\Delta H^\circ$  is independent of  $\alpha$ , the  $\Delta G^\circ$ , hence  $K$ , decreases with the increasing  $\alpha$ .<sup>44</sup>

For the protonation of  $(\text{ZH}_2^{+-})$  **13** to  $(\text{ZH}_3^{++})$  **19** (Scheme 3), the latter is more hydrated thus having expanded polymer chain as evinced by its greater viscosity value (*cf.* Fig. 3b-v vs. 3b-ii). The more exposed RU makes the neutralization process easier with the increasing  $\alpha$  (Fig. 3c,  $i = 3$ ).<sup>45,46</sup> With increasing  $\alpha$ , increasing imbalance in favour of positive charge also increases

the degree of hydration which leads to greater entropy changes because of release of a greater number of molecules during progressive protonation.

### 3.6 Scale inhibition study

In a Reverse Osmosis (RO) process, feed water is converted to product water and rejects brine, in which supersaturation of dissolved salts, like  $\text{CaSO}_4$  and  $\text{CaCO}_3$ , may lead to precipitation which reduces the efficacy of the membrane separation process.

The percent scaling inhibition (PSI) is calculated using eqn (4):

$$\text{PSI} = \frac{[\text{Ca}^{2+}]_{\text{inhibited}(t)} - [\text{Ca}^{2+}]_{\text{blank}(t)}}{[\text{Ca}^{2+}]_{\text{inhibited}(t_0)} - [\text{Ca}^{2+}]_{\text{blank}(t)}} \times 100 \quad (4)$$

where  $[\text{Ca}^{2+}]$  concentrations are used at time zero and  $t$ . The inhibited and blank are used to describe the presence and absence of the antiscalant.

The concentration of  $\text{Ca}^{2+}$  and  $\text{SO}_4^{2-}$ , present in the reject brine of a RO plant,<sup>47</sup> was described as 1-CB (concentrated brine). The scaling behavior in the presence of PA **13** was carried out in a supersaturated solution of  $\text{CaSO}_4$  comprising 3-CB



**Table 4** Percent scale inhibition in the presence of PA 13 in 3 CB<sup>a</sup> supersaturated CaSO<sub>4</sub> solution at 40 °C

Entry	Sample (ppm)	Percent inhibition at times (min)						
		50	100	200	300	400	500	700
1	5	100	92	71	24	22	17	17
2	10	100	100	88	81	76	71	63
3	15	100	99	96	91	88	83	75
4	20	100	100	100	100	100	100	98

<sup>a</sup> Three times the concentration of Ca<sup>2+</sup> and SO<sub>4</sub><sup>2-</sup> found in the concentrated brine of an RO plant.

concentration of Ca<sup>2+</sup> (2600 ppm) and SO<sub>4</sub><sup>2-</sup> (6300 ppm) by conductivity measurements. A sudden drop in the conductivity indicates the onset of CaSO<sub>4</sub> scaling (Fig. 3d).

It is indeed satisfying that in the presence of 5 and 20 ppm 13, a 100% scale inhibition was registered for about 50 and 500 min, respectively (Table 4). Since the reject brine usually has a residence time of ≈ 30 min in the osmosis chamber, the current antiscalant may thus be very effective in inhibiting CaSO<sub>4</sub> scaling. As shown in Fig. 3d, the onset of precipitation occurs after an induction period; an accelerated growth of CaSO<sub>4</sub> crystals is indicated by a sudden drop in conductivity. For a duration of 700 min, 20 ppm PA 13 did not show any induction time. The crystal growth starts after nucleation process, which is interfered with the complexation of the metal ions by the chelating ligands of the antiscalant.<sup>48,49</sup> The gypsum scale, *i.e.*, CaSO<sub>4</sub> in mineral form, occurs during several processes involving production of water.<sup>50</sup> PA 13 is found to be remarkably efficient in preventing scale formation, and as such it has the ability to mitigate the membrane fouling in RO plants.

## 4. Conclusions

Several diallylamine derivatives 1a, b, 5 and 7 as well as quaternary diallyldialkylammonium chlorides 15a, b has been terpolymerized with MA and SO<sub>2</sub> using APS initiator or UV light at a λ of 365 nm in an attempt to obtain amine (salt)-MA-SO<sub>2</sub> terpolymer. In contrast to reported literature, only 1–2 mol% of MA was incorporated into the polymer chain mainly consisting of amine (salt)-SO<sub>2</sub> copolymers. The non-incorporation of MA is attributed to the far greater rate of propagation of amine (salt)-SO<sub>2</sub> than either amine (salt)-MA or MA-SO<sub>2</sub> under the polymerization conditions. The reactivity ratios of both monomers in the amine (salt)-MA and MA-SO<sub>2</sub> pairs are ≈ 0; however, in a three-monomer system: amine (salt)-MA-SO<sub>2</sub>, the very slow reactivity of MA does not allow its incorporation into terpolymer chain to any meaningful extent.

The 1c-MA copolymer PA 13 has been synthesized in excellent yield with an anticipation that it could be a potential antiscalant. Under pH-induced changes, stimuli-responsive polyampholyte 13 was transformed to cationic 19, polyampholyte-anionic 20, and dianionic polyelectrolyte 21 to examine their viscosity. The viscosity values of 13 in the presence of salt NaCl confirmed its antipolyelectrolyte behaviour. The log *K* (*i.e.* p*K*<sub>a</sub>) of two carboxylic acid groups and NH<sup>+</sup> in 13

has been determined to be 2.62, 5.59, and 10.1, respectively. PA 13 was evaluated as an antiscalant for potential application in reverse osmosis (RO) plants. At concentrations of 5 and 20 ppm, it demonstrated remarkable efficiency of ≈ 100% for CaSO<sub>4</sub> scale inhibition from its supersaturated solution for 50 and 500 min, respectively. Since an antiscalant should be effective for the duration of brine's residence time (≈ 30 min) in the osmosis chamber, the synthesis of PA 13 in excellent yields from cheap starting materials and its very impressive performance may accord it a prestigious place among many an environment-friendly phosphate-free antiscalant. Note that polyphosphate additives used for controlling scale formation, when discharged in the sea have deleterious influence over the marine biota picture.<sup>51</sup>

## Conflicts of interest

There are no conflicts to declare.

## Acknowledgements

The facilities provided by KFUPM are gratefully acknowledged.

## References

- G. B. Butler, *Cyclopolymerization and Cyclocopolymerization*, Marcel Dekker, New York, 1992.
- S. Kudaibergenov, W. Jaeger and A. Laschewsky, *Adv. Polym. Sci.*, 2006, **201**, 157–224.
- A. Laschewsky, *Polymers*, 2014, **6**, 1544–1601.
- P. K. Singh, V. K. Singh and M. Singh, *e-Polym.*, 2007, **30**, 1–34.
- G. B. Butler, *J. Polym. Sci., Part A: Polym. Chem.*, 2000, **38**, 3451–3461.
- F. C. McGrew, *J. Chem. Educ.*, 1958, **35**, 178–186.
- N. Y. Abu-Thabit, I. W. Kazi, H. A. Al-Muallem and S. A. Ali, *Eur. Polym. J.*, 2011, **47**, 1113–1123.
- S. A. Ali, H. A. Al-Muallem and M. A. J. Mazumdar, *Polymer*, 2003, **44**, 1671–1679.
- S. A. Ali, I. B. Rachman and T. A. Saleh, *Chem. Eng. J.*, 2017, **330**, 663–674.
- F. Rullens, M. Devillers and A. Laschewsky, *Macromol. Chem. Phys.*, 2004, **205**, 1155–1166.
- I. Y. Yaagoob, H. A. Al-Muallem and S. A. Ali, *RSC Adv.*, 2017, **7**, 31641–31653.
- E. Kogure, N. Morii, Y. Makino, T. Hawakawa and K. Tsukuda, JP Pat., 2007106920 A 20070426, 2007.
- Y. Yomogida and H. Torigoe, JP Pat., 2012214539 A 20121108, 2012.
- N. Suzuki, H. Togashi, S. Ito and Y. Yamazaki, JP Pat., 2007238921 A 20070920, 2007.
- S. A. Ali, N. Y. Abu-Thabit and H. A. Al-Muallem, *J. Polym. Sci., Part A: Polym. Chem.*, 2010, **48**, 5693–5703.
- O. C. S. Al-Hamouz and S. A. Ali, *J. Polym. Sci., Part A: Polym. Chem.*, 2012, **50**, 3580–3591.
- S. A. Ali, I. W. Kazi and N. Ullah, *Ind. Eng. Chem. Res.*, 2015, **54**, 9689–9698.



- 18 S. H. Pine, *J. Chem. Educ.*, 1968, **45**, 118.
- 19 Y. Negi, S. Harada and O. Ishizuka, *J. Polym. Sci., Part A: Polym. Chem.*, 1967, **5**, 1951–1965.
- 20 S. A. Ali, I. W. Kazi and F. Rahman, *Polym. Int.*, 2014, **63**, 616–625.
- 21 S. A. Ali and O. C. S. Al-Hamouz, *Polymer*, 2012, **53**, 3368–3377.
- 22 S. A. Haladu and S. A. Ali, *J. Polym. Sci., Part A: Polym. Chem.*, 2013, **51**, 5130–5142.
- 23 A. I. Vorobeve, G. R. Sultanova, A. K. Bulgakov, V. I. Zainchkovskii and S. V. Kolesov, *Pharm. Chem. J.*, 2013, **46**, 653–655.
- 24 S. Harada and K. Arai, *US Pat.*, 3585118, 1971.
- 25 S. A. Ali, Y. Umar and B. F. Abu-Sharkh, *J. Appl. Polym. Sci.*, 2005, **97**, 1298–1306.
- 26 A. I. Vorobeve, E. V. Vasileva, K. A. Gaisina, Y. I. Puzin and G. V. Leplyanin, *Polym. Sci., Ser. A*, 1996, **38**, 1077–1080.
- 27 J. C. Salamone, W. Volksen, A. P. Olson and S. C. Israel, *Polymer*, 1978, **19**, 1157–1162.
- 28 T. A. Wielema and J. B. F. N. Engberts, *Eur. Polym. J.*, 1987, **23**, 947–950.
- 29 V. M. M. Soto and J. C. Galin, *Polymer*, 1984, **25**, 254–262.
- 30 M. Galin, A. Chapoton and J.-C. Galin, *J. Chem. Soc., Perkin Trans. 2*, 1993, 545–553.
- 31 A. W. Lloyd, C. J. Olliff and K. L. Rutt, *Int. J. Pharm.*, 1996, **131**, 257–262.
- 32 Z. E. Ibraeva, M. Hahn, W. Jaeger, L. A. Bimendina and S. E. Kudaibergenov, *Macromol. Chem. Phys.*, 2004, **205**, 2464–2472.
- 33 G. B. Butler and R. J. Angelo, *J. Am. Chem. Soc.*, 1957, **79**, 3128–3131.
- 34 R. M. Pike and R. A. Cohen, *J. Polym. Sci.*, 1960, **44**, 531–538.
- 35 S. A. Ali, A. Rasheed and M. I. M. Wazeer, *Polymer*, 1999, **40**, 2439–2446.
- 36 V. D. Vynck and E. J. Goethals, *Macromol. Rapid Commun.*, 1997, **18**, 149–156.
- 37 M. Hahn, W. Jaeger, R. Schmolke and J. Behnisch, *Acta Polym.*, 1990, **41**, 107–112.
- 38 K. Nishida, K. Kaji, T. Kanaya and N. Fanjat, *Polymer*, 2002, **43**, 1295–1300.
- 39 M. Gao, K. Gawel and B. T. Stokke, *Eur. Polym. J.*, 2014, **53**, 65–74.
- 40 Z. Cao and G. Zhang, *Phys. Chem. Chem. Phys.*, 2015, **17**, 27045–27051.
- 41 S. Morozova, G. Hu, T. Emrick and M. Muthukumar, *ACS Macro Lett.*, 2016, **5**, 118–122.
- 42 R. Barbucci, M. Casolaro, N. Danzo, V. Barone, P. Ferruti and A. Angeloni, *Macromolecules*, 1983, **16**, 456–462.
- 43 M. S. Bodnarchuk, K. E. B. Doncom, D. B. Wright, D. M. Heyes, D. Dini and R. K. O'Reilly, *RSC Adv.*, 2017, **7**, 20007–20014.
- 44 R. Barbucci, M. Casolaro, P. Ferruti and M. Nocentini, *Macromolecules*, 1986, **19**, 1856–1861.
- 45 R. Barbucci, M. Casolaro, M. Nocentini, S. Correzzi, P. Ferruti and V. Barone, *Macromolecules*, 1986, **19**, 37–42.
- 46 A. Fini, M. Casolaro, M. Nocentini, R. Barbucci and M. Laus, *Makromol. Chem.*, 1987, **188**, 1959–1971.
- 47 F. H. Butt, F. Rahman and U. Baduruthamal, *Desalination*, 1995, **103**, 189–198.
- 48 H. David, S. Hilla and S. Alexander, *Ind. Eng. Chem. Res.*, 2011, **50**, 7601–7607.
- 49 R. J. Davey, *The Role of Additives in Precipitation Processes, Industrial Crystallization, Proc. Symp.*, ed. S. J. Jancic and E. J. de Jong, North-Holland Publishing Co., 8th edn, 1982, pp. 123–135.
- 50 G. Mazziotti di Celso and M. Prisciandaro, *Desalin. Water Treat.*, 2013, **51**, 1615–1622.
- 51 A. M. Shams El Din, Sh. Aziz and B. Makkawi, *Desalination*, 1994, **97**, 373–388.

